IASJ المجلات الاكاديمية العراقية

Tikrit Journal of Pure Science

ISSN: 1813 – 1662 (Print) --- E-ISSN: 2415 – 1726 (Online)

Journal Homepage: http://tjps.tu.edu.iq/index.php/j

Characterization of the Carbonate Reservoir Unit A of the Upper Triassic Kurra Chine Formation in the well SH-4, Shaikan Oilfield, Iraqi Kurdistan Region, Using Wireline Log Data

Dler H. Baban , Mostafa M. Ahmed

Geology Department, College of Sciences, Sulaimani University, Sulaimani, Iraq

DOI: http://dx.doi.org/10.25130/tjps.26.2021.031

ARTICLE INFO.

Article history:

-Received: 10 / 10 / 2020

-Accepted: 3 / 12 / 2020

-Available online: / / 2021

Keywords: Shaikan, Kurra Chine, Reservoir Units, Flow Zone Indicator.

Corresponding Author:

Name: Dler H. Baban

E-mail:

Tel:

ABSTRACT

Unit A of Kurra Chine Formation has been studied in the well Shaikan - 4 (SH-4) at Shaikan Oilfield in Northern Iraqi Kurdistan Region. The available conventional wireline log data and the existed core test values have been used to characterize the reservoir properties of the studied unit and to determine the flow efficiency of the reservoired fluids. The dolomite and anhydrite dominated lithology of the studied unit contains low percentages of shale except the upper most part of the unit in which shale content exceeds 30%. The porosity is less than 5% in most parts of the unit and secondary porosity comprises less than 4% of the total porosity in some horizons. The shale content consists primly of Illite and Chlorite and distributes in a dispersed pattern. Hydrocarbons are exist almost along the studied unit in saturations exceeding 70% at the middle and lower part of the unit. No effective permeable intervals observed at the upper part of the unit, whereas permeable zones of greater than 70mD are observed at the lower part. Three reservoir units distinguished in Kurra Chine A unit based on variations in shale content, porosity, and permeability. The studied unit contains four distinctive types of Hydraulic Flow Units (HFU) of less than 2.0, 20-5.5, 5.5-10, and greater than 10 Flow Zone Indicator (FZI) values. The calculated net to gross pay ratio for the studied Kurra Chine A Unit appeared to be about 28% representing the collective 52m net pay to the 184m gross thickness of the studied A Unit.

Introduction

The Shaikan Field is one of the largest oil discoveries in the Kurdistan Region of Iraq and has been in production since July 2013.

Shaikan Oilfield is located about 85 kilometers northwest of the regional capital Erbil and about 60 km south-east of the Duhok City (Fig.1). The field was discovered by Gulf Keystone Petroleum (GKP) and MOL's subsidiary (Kalegran), and it is one of the largest fields in Kurdistan, with majority of the oil currently being produced from the Upper Jurassic fractured carbonates [1].

Moderately heavy oil of 18 – 22^{0}API and low GOR discovered in the Cretaceous Sarmord Formation and the Jurassic Barsarin, Sargelu, Alan, Mus, and Butmah formations [1]. Light oil with GOR greater than 1000scf/bbl (43^{0}API) discovered in the upper part of Kurra Chine Formation (Unit A) when the first well drilled by Gulf Keystone Oil Company in 2009, whereas the middle part of the formation (Unit B) appeared containing gas condensate of 100 – 450 bbl/mmcf (54^{0}API) [1].

Most of the studies about Kurra Chine Formation outside Kurdistan Region are source rock evaluation studies considering the formation as a possible source rock [2][3][4][5]. The exploration activities that took place in Kurdistan Region after 2003, and the drilling operations since that time indicated Kurra Chine Formation is mostly as a reservoir rather than a source. In contrast to the other parts of Iraq, Kurra Chine Formation in Kurdistan Region is generally located at shallower depths and more easily can be reached and drilled (although the high reservoir pressure remains a great challenge to be overcome). The formation already drilled or planed as a target to

be drilled in a number of discovered oilfields in the region such as Sangaw, Bina Bawea, Swara Tika, Atrush, Shaikan, Sheikh Adi, Bakrman, Barda Rash, Simrit, Mirawa, Shakrok …etc.

In this study, the reservoir properties of the Unit A of Kurra Chine Formation are tried to be characterized using data of wireline logs from a selected well (SH-4) of Shaikan Oilfield.

Kurra Chine Formation:

Kurra Chine Formation is the most widespread formation of the late Triassic sequence in Iraq. It was firstly defined by Wetzel in 1950 [6] from the northern thrust zone of Northern Iraq where it comprises monotonous dark brown and black limestone. The formation as described in its type section at Ora in Iraqi Kurdistan, is generally composed of dark and brown limestones alternating with papery shale and dolomites [7]. At the subsurface, the formation contains thick evaporite intervals and consists of alternating limestones, dolomites, shale, anhydrite and some halite [8].

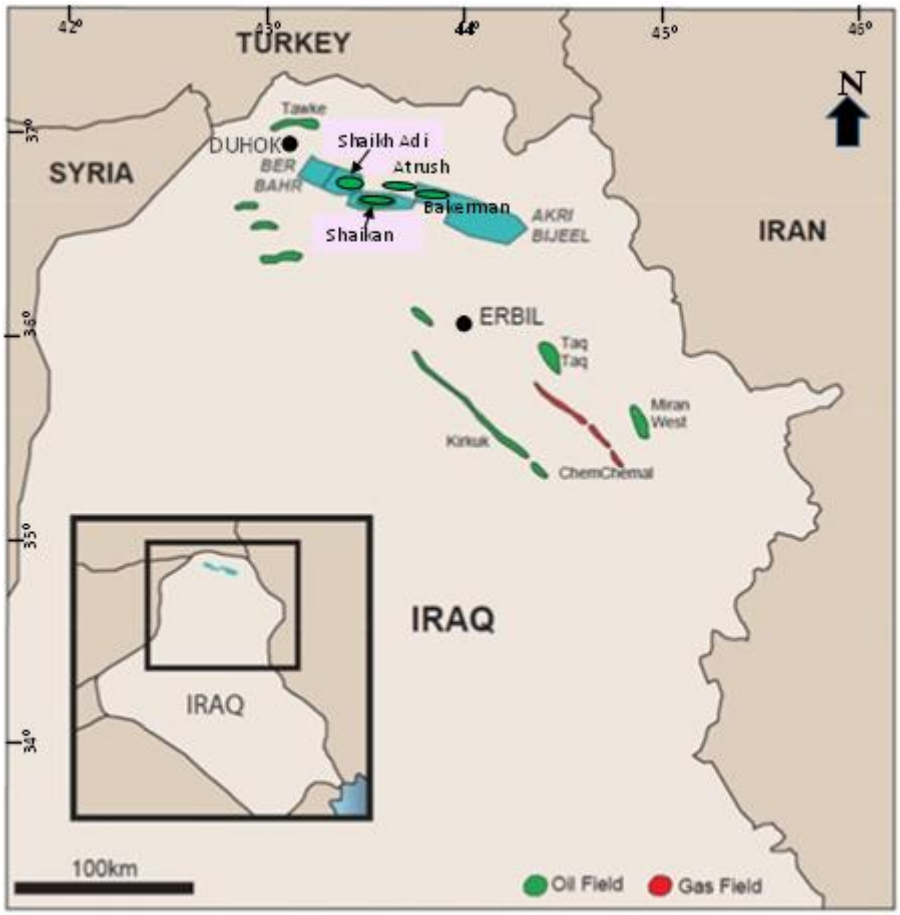

Fig. 1: Location map of the studied Shaikan Oilfield (modified after[1]).

According to [9], two carbonate units and two overlying evaporite members are known in the subsurface. The carbonates are representing the Tr60 and Tr70 Main Flooding Surfaces (MFS) of [10] and their subsequent highstands system track, whereas, the evaporites are representing lowstand system track deposits at the base of the sequences Tr70 and Tr80.

The outcropped upper part of the formation in the type section is believed to be of Upper Triassic (Rhaetian) age [6]. The basal part of the formation in the wells KH 5/4, KH5/8, and KH5/9 is reported by [4] and [11] as of Carnian age.

[12] mentioned that Kurra Chine Formation deposited in an inner shelf to restricted lagoon/sabhka environment. The upper carbonate dominated part of the formation is deposited in an epeiric platform dominated by shallow subtidal and supratidal cycles with local sabkhas [9]. The thickness of the formation at the type section is up to 850m, and according to [2] the thickness ranges between less about 500m and greater than 1000m at the subsurface (Fig.2).

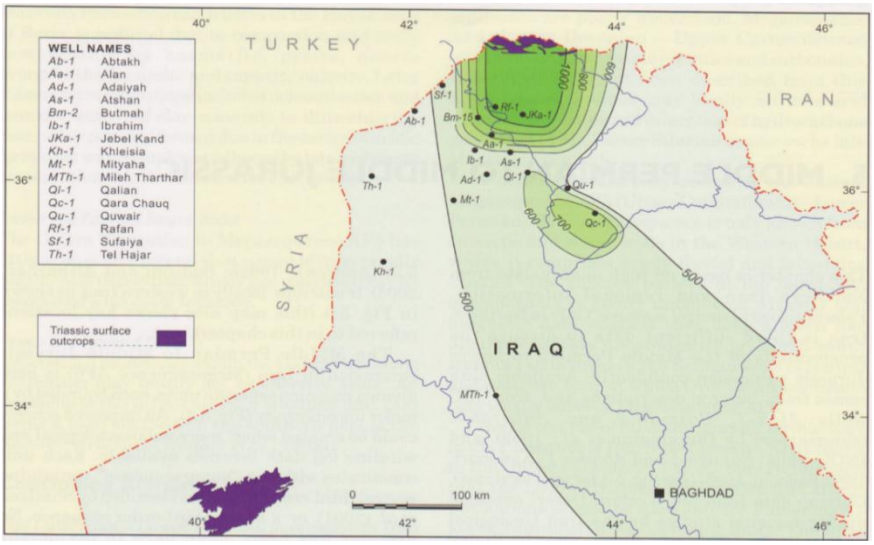

Fig. 2: Isopach map of the Kurra Chine Formation at central and northern Iraq (after [9] based on [2]).

Siliciclastic reservoir intervals occur locally in Kurra Chine Formation and believed to be generally of poor reservoir quality. The formation appeared to be containing oil in northwestern Iraq at Alan, Sufaiyah, and Butmah oilfields [9].

According to [2], Kurra Chine Formation contains source and reservoir rock intervals in Northern Iraq. [4] confirmed the source potentiality of the formation through a geochemical analysis for selected samples of the formation in Jabal Kand-1 well and recorded up to 5% Total Organic Carbon (TOC) values. The mudstones which interbedded with the anhydrites in the formation are believed to represent potential source rocks [9].

[2] mentioned that the anhydrites at the lower part of the formation seals the underlying carbonate reservoirs in Alan, Adaiyah, and Ibrahim areas northwest Iraq.

Kurra Chine Formation is disconformably rests on the Gali Khanah Formation at the type section [7]. The upper boundary is not so clear in some areas like Sirwan [8] but at the type area, the contact is gradational and conformable with the overlying Baluti Formation.

Lately, the formation subdivided by the operated oil companies in Kurdistan to three units namely A, B, and C representing, upper, middle, and lower parts of the formation respectively. Kurra Chine A composed mainly of anhydrite beds being subdivided by dolomites and mudstones. The mudstone is much dominated at the upper part of this unit. Kurra Chine B on the other hand composed primly of dolomite, dolomitic anhydrite, dolomitic limestone and anhydrite, with mudstones especially at the lower part of this unit. Kurra Chine C is composed mainly of anhydrite with limestone, dolomitic anhydrite, and dolomite.

Tectonic Setting and Stratigraphy:

Shaikan structure tectonically locates within the Zagros Fold Belt (Kirkuk Embayment) and arranged as an echelon pattern anticlines with Shaikh Adi, Atrush, and Bakerman structures (Fig.1). The structure is among those anticlines which have the Taurus trend of folding with an E-W axis direction. The general idea about the Taurus trend structures in Northern Iraq is that they developed on detached thrust sheets and/or formed over basement-involved faults (just like Zagros trend folds) [13].

[13] suggested that the gravity lows and sedimentary thickenings of the Taurus trend anticlines are due to being forced folds overlying the Permo-Triassic grabens that were inverted by compression during continental collision between the Eurasian and the African-Arabian plates which began in the mid-Tertiary and culminated during Late Miocene to Pliocene time.

[14] believe that Shaikan Anticline is located over and parallel to a listric fault in the basement rocks and cut through the sedimentary cover by normal sense of movement. Reactivation of this fault was basically responsible for the geometrical configuration of the Shaikan Anticline.

Kurra Chine Formation deposited during Upper Triassic when the province that is now northern Iraq was a rifting margin and later transitioning to a passive margin during late Mesozoic to mid-Tertiary time.

The Injanah Formation of Late Miocene age represents the youngest among the outcropped surface rocks at Shaikan Oilfield, followed by the Fatha, Pila Spi, Gercus, Sinjar, Kolosh, Aqra, Shiranish, and Bekhmah formations. The Cretaceous rocks at the location of the studied well (SH-4) start with the reefal limestone of the Maastrichtian Aqra Formation followed by the Campanian – Maastrichtian marl and marly limestone of the Shiranish Formation. Figure 3 shows the succession from Sinjar Formation as penetrated by SH-4 well in Shaikan Oilfield with the depth of the top of the formations (starting from top of Kolosh Formation) till the total depth of the well at 3386m.

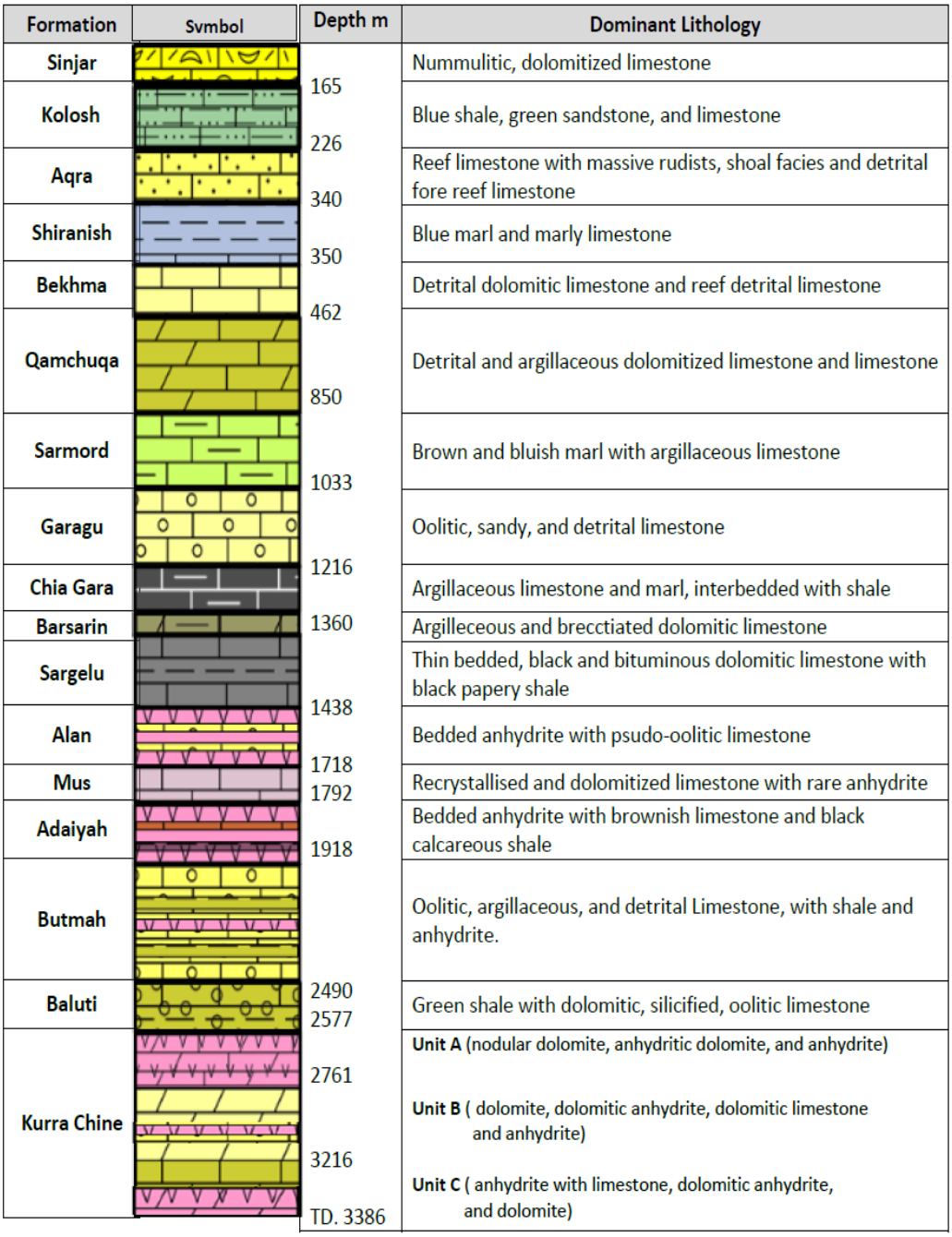

Fig. 3: Stratigraphic column for SH-4 well, Shaikan Field) (after [1]).

Data and Methodology:

The available wireline log data of the Unit A of Kurra Chine Formation has been used in this study for characterizing the main reservoir properties of the upper part of the formation. The selected well of the study (SH-4), is located at the western plunge of Shaikan structure (Fig.4) and penetrated Kurra Chine (A) between depths 2577m and 2761m.

The used logs in this study and the main purposes of using each ones are shown in Table 1.

Data of core test for a selected interval between depths 2642m and 2655m also used for calculating permeability for the entire studied section through the fuzzy method of Multiple Regression Analysis.

The conventional and standard methods of well log analysis have been followed for obtaining the necessary reservoir properties of the studied formation starting with checking the data and digitizing the log plots by Neural Log software.

Replotting the digitized logs done using Excel, Grapher, and Logplot softwares. Some of the reservoir properties obtained directly through observing the log plots (ex. shaley, evaporitic, and permeable zones) and other properties through cross over of different logs (ex. gas bearing zones). Standard equations and different crossplots used for correction purposes and for obtaining the requested essential reservoir parameters.

Fig. 4: Location of the study well on Shaikan Oilfield (after [15]).

Table1: The used logs in this study and purposes of their use.

#	Log Type	Main purposes of use
1	Caliper	Checking borehole wall condition (enlargement, on gauge, or mudcake creation) for detecting type of lithology, existence of permeable zones, and calibrating the reliability of the other log type readings.
2	Gamma Ray (GR)	Detecting lithology and calculating shale volume
3	Spectral Gamma Ray (SGR)	Detecting clay minerals composing the shale
4	Sonic Log (Borehole Compensated type BHC)	Detecting lithology and calculating secondary porosity
5	Formation Density Log (FDC)	Detecting lithology and type of shale distribution, calculating primary and secondary porosity, detecting gas zones
6	Compensated Neutron Log (CNL)	Detecting lithology and type of shale distribution, calculating primary and secondary porosity, detecting gas zones
7	Resistivity logs: Laterolog Deep (LLD); Laterolog Shallow (LLS); and Microspherical Focused Log (MSFL)	Calculating water saturation and detecting hydrocarbon bearing zones

Lithology Determination:

Most of the conventional wireline logs aid in determining lithology of the logged intervals especially gamma ray and porosity logs. Figure 5 shows the ρb – $Ø_N$ crossplot of Sclumberger Company (1988) by which the dominant lithology of the studied Kurra Chine (A) has been detected. The lithology (as expected) looks to be composed mainly of anhydritic dolomite, anhydrite, and dolomite. The existence of shale intervals also can be detected from the sample points located at the shale region of the crossplot (at the right side).

The M-N crossplot for lithology determination also applied in this study depending on the values of the three known porosity logs of sonic, density, and neutron. Both M and N factors can be calculated using Equations Eq.1 and Eq.2 respectively. Additional benefit of this crossplot on ρb – $Ø_N$ crossplot is better identification of the secondary porosities and that due to contribution of sonic porosity also in this method.

$$M = \frac{\Delta tfl - \Delta t}{\rho b - \rho fl} * 0.01 \quad \text{------ Eq.1}$$

$$N = \frac{ØNfl - ØN}{\rho b - \rho fl} \quad \text{-------- Eq.2}$$

Where:

Δtfl: Interval transit time in the mud filtrate (189μsec/ft for fresh mud, the case of this study)

Δt: Interval transit time in the formation (from log)

ρb: Formation bulk density(from log)

ρfl: Fluid density (1.0 g/cc for fresh mud, the case of this study)

ØNfl: Neutron porosity of the fluid (usually 1.0)

ØN: Neutron porosity (from log)

The multiplier 0.01 is used to make the M values compatible for easy scaling.

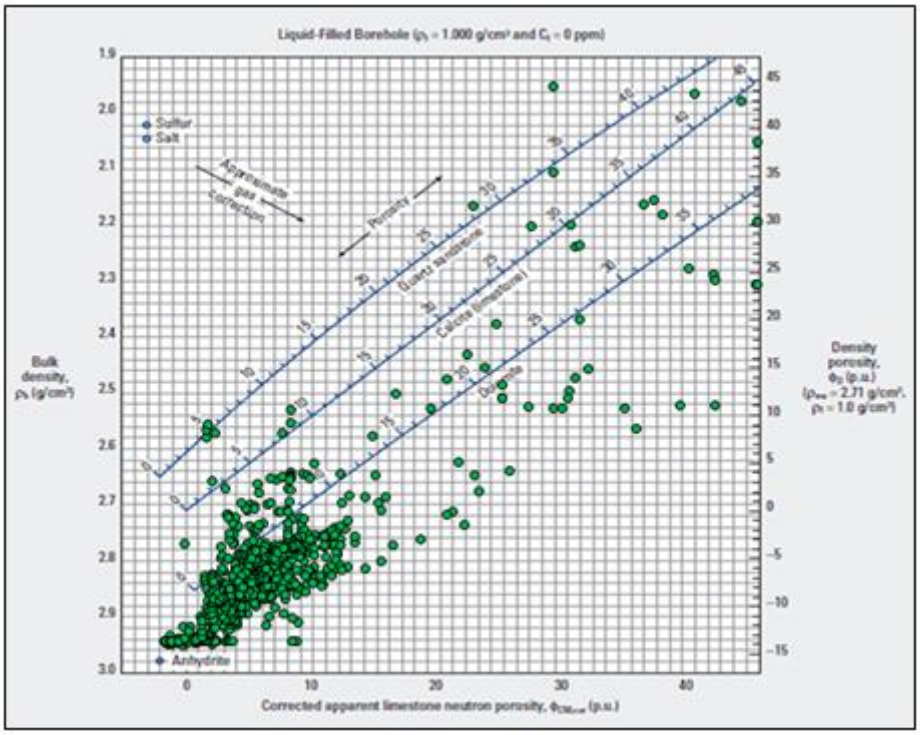

Fig. 5: Neutron-Density cross plot for determining lithology of the Kurra Chine A Unit in the well SH-4.

Domination of dolomite and anhydrite also approved by the M-N crossplot in addition to observing the effect of secondary porosities on scattering the sample points towards the upper side of the crossplot.
It's important to mention that the results of the both used lithology determination crossplot is totally coincides with the general composition of the Kurra Chine A unit suggested by KGS the operator company of Shaikan Oilfield (Fig. 7).
According to GKS, about 28% of Kurra Chine (A) in the SH-4 well is composed of anhydrite and 23% of different types of dolomite, in addition to 42% of anhydritic dolomite and dolomitic anhydrite. Shale (mudstone) comprises only 3% of the total lithology.

Shale Volume Calculation:

Although the studied Kurra Chine A looks to be containing low percentage of shale, but still determining the shale and shaly intervals is vital for either considering the permeable zones or for correcting the calculated porosities.

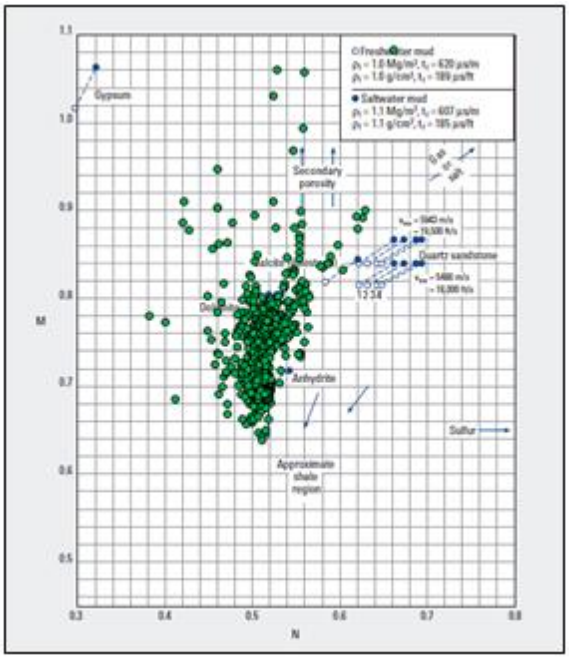

Fig. 6: M-N cross plot for determining lithology of the Kurra Chine A Unit in the well SH-4.

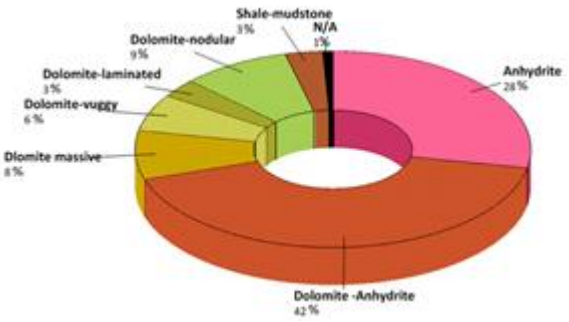

Fig. 7: Pie distribution of the lithology components of the Kurra Chine A Unit in the well Sh-4.

Gamma ray log considers the best for determining shale volume in reservoirs. The sensed gamma radiations by the tool are primly sourced from radioactive elements of Potassium (K^{40}), Uranium (U^{235}) and Thorium (Th^{232}) which all are exist within the clay minerals of the shale. Accordingly, the intensity of the sensed gamma radiation is proportional to the volume of the radioactive minerals and their ages or generally to the volume of shale.

The shale volume calculated for the studied Kurra Chine A unit through firstly, calculating Gamma Ray Index (GRI) (Eq.3) and secondly, calculating shale volume using the equation suggested by [16] for shale volume calculation in consolidated rocks older than Tertiary (Eq.4).

$$GRI = \frac{GRlog - GRmin}{GRmax - GRmin} \text{ ---------- Eq.3}$$

$$Vsh = 0.33\ [2^{(2*GRI)} - 1.0] \text{ ------ Eq.4}$$

Where:

GRI: Gamma ray index

GRlog: Gamma ray reading from log (at any depth)

GRmin: Minimum gamma ray reading (from log at a clean zone)

GRmax: Maximum gamma ray reading (from log at a shale zone)

Vsh: Volume of shale

Figure 8A shows the gamma ray record and the calculated shale volume for Kurra Chine A unit in SH-4.

Figure 8B shows that shale content of Kurra Chine A Unit in SH-4 is generally increases upward from less than 3% at the lower part of the unit to about 5% at the middle part and greater than 25% at the upper most part of the unit. Thus, the lower and middle parts of Kurra Chine A

Unit can be considered as clean from shale content point of view, whereas the upper part is more likely to be considered as shaly. The obvious fluctuations in the shale content at the upper part indicates interbeding shaley intervals with anhydrite or dolomitic anhydrite intervals.

Increasing shale content at the upper part is mostly due to the change in the depositional environment and become more close to the lagoonal and estuarine depositional environment of Baluti Formation [10] [11].

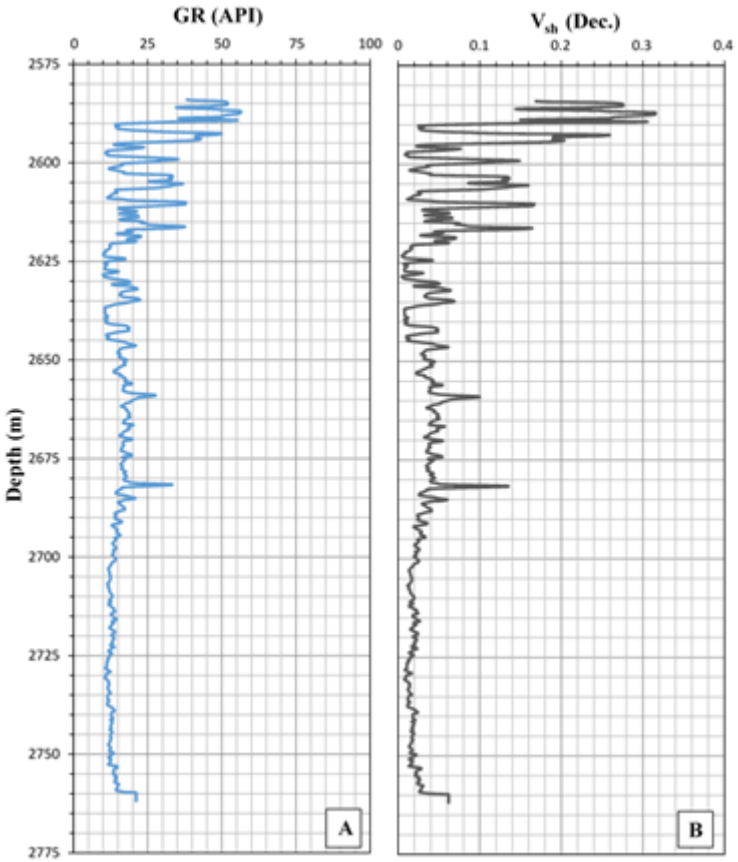

Fig. 8: A; Gamma ray record and B; calculated shale volume for Kurra Chine A Unit in SH-4.

The gradual upward increase of the shale content also indicate deepening upward of the paleo-depositional environment of Kurra Chine A.

The record of the Spectral Gamma Ray log (SGR) for the studied unit (Fig. 9) shows the same trend of increase for the radioactive elements of Thorium (Th), Uranium (U) and Potassium (K) from the lower part of the unit towards the top. No obvious variations seen between the ratios of the three mentioned radioactive elements indicating to no obvious change in the types of the clay minerals composing the shale. Illite looks to be the dominated clay mineral of the shale content in addition to the Chlorite in a less percentage (Fig.10). According to [17], Illite and Chlorite most the time are dispersed in the form of pore bridging and pore lining in the subsurface and affect both porosity and permeability of the rock.

It's worth to mention that the relative increase of the Uranium content at the depth interval 2640 - 2680m is an indication to being the shale at this interval of high organic matter content (zone of hydrocarbon generation) [17].

Porosity Calculation:

Porosity has been calculated for the studied unit through sonic, density, and neutron porosity logs. The recorded interval transit time (Δt) of the sonic log and bulk density (ρb) of density log were converted to porosity values using equations Eq.5 and Eq.6 respectively.

$$Øs = \frac{\Delta tlog - \Delta tmat}{\Delta tfl - \Delta tmat} \text{ ---------Eq.5}$$

Where:

Øs: Sonic porosity

Δtlog: Travel transit time at any depth in μsec/ft (from the log)

Δtmat: Travel transit time at the matrix in μsec/ft (43.5 for dolomite and 50 for anhydrite, the cases of this study)

Δtfl: Travel transit time at the mud filtrate in μsec/ft (189 for fresh water, the case of this study)

$$ØD = \frac{\rho mat - \rho b}{\rho mat - \rho fl} \text{ -------- Eq.6}$$

Where:

ØD: Density porosity

ρmat: Density of the matrix in gm/cc (2.87 for dolomite and 2.98 for anhydrite, the cases of this study)

ρlog: Bulk density at any depth in gm/cc (from the log)

ρfl: Density of the mud filtrate in gm/cc (1.0 for fresh water, the case of this study)

Correction from shale impact done for the three porosities of ØS, ØD, and ØN through applying the suggested formulas by [19], Eq.7-9 respectively (Fig. 11).

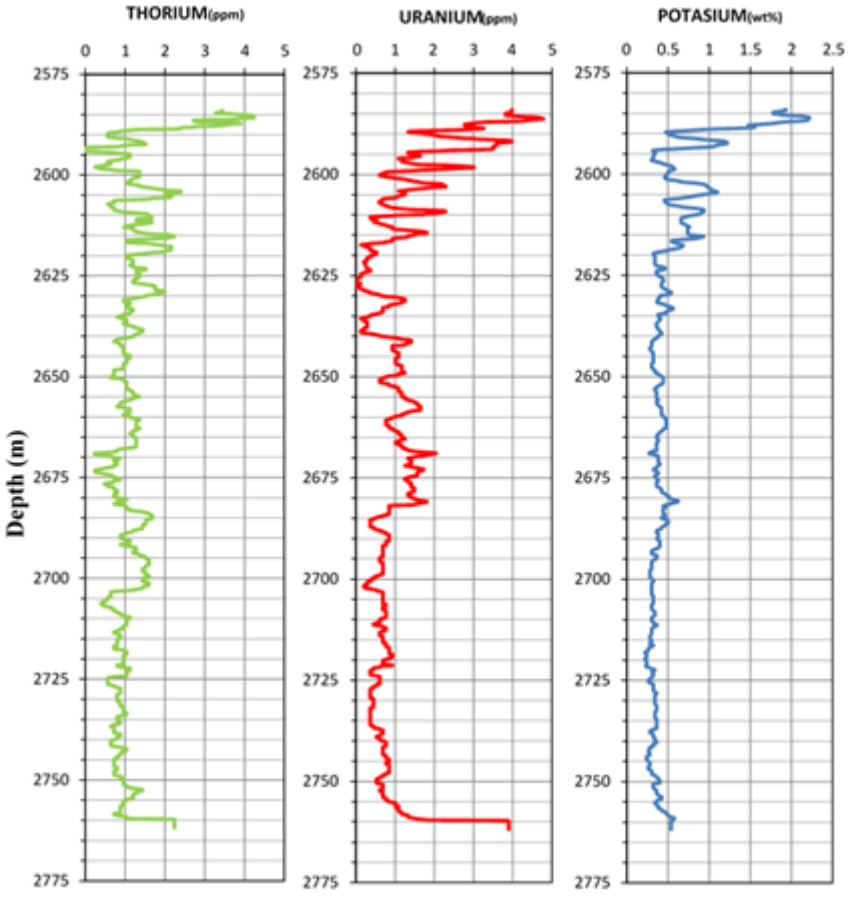

Fig. 9: Record of the Spectral Gamma Ray (SGR) log data (Thorium, Uranium, and Potassium curves) for the Kura China Formation A Unit in the well SH-4.

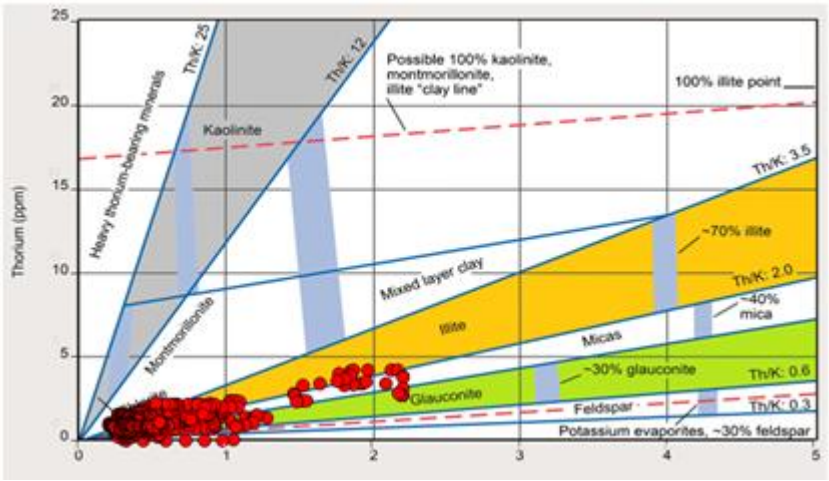

Fig. 10: Thorium - Potassium crossplot for identification of the clay minerals composing the shale content of the Kura China A Unit in the well SH-4 (The crossplot is after [18]).

$\emptyset Scorr = \emptyset S - (Vsh * \emptyset Ssh)$---------- Eq.7
$\emptyset Dcorr = \emptyset D - (Vsh * \emptyset Dsh)$-------- Eq.8
$\emptyset Ncorr = \emptyset N - (Vsh * \emptyset Nsh)$-------- Eq.9
Where:
ØScorr: Sonic porosity corrected from shale impact
ØS: Sonic porosity (incorrected)
Vsh: volume of shale
ØSsh: Sonic porosity for adjacent shale
ØDcorr: Density porosity corrected from shale impact
ØD: Density porosity (incorrected)
ØDsh: Density porosity for adjacent shale
ØNcorr: Neutron porosity corrected for shale impact
ØN: Neutron porosity (incorrected)
ØNsh: Neutron porosity for adjacent shale

The porosity of Kurra Chine A Unit as shown in Figure 11 is less than 10% in most parts of the unit, except the uppermost part where in some depth intervals the porosity exceeded 25%. It's important to mention that the calculated high porosity at the uppermost part of the formation is not reliable due to the enlargement occurred to the borehole wall and been observed by the caliper log. Such observable enlargement is definitely affected the recorded values of the porosity logs.

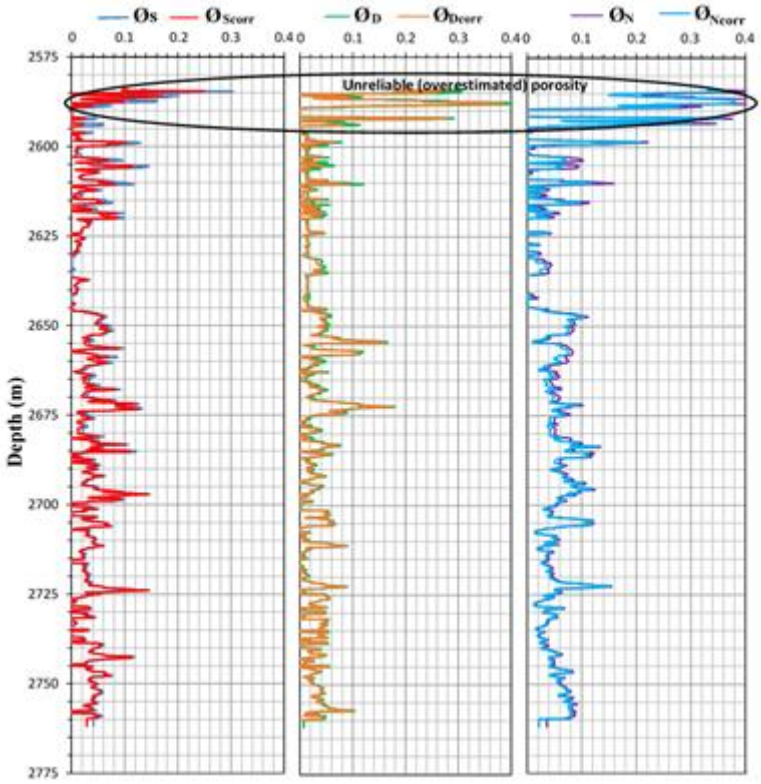

Fig. 11: Incorrected and corrected Sonic, Density, and Neutron porosities for Kurra Chine A Unit in SH-4.

As the three types of the porosity logs are affected by the borehole condition, lithology, and fluid content in different ways, so most the time the corrected Neutron-Density combination porosity (ØNDcorr) considers the best for evaluation of porosity for logged reservoirs.

The calculated ØNDcorr by equation Eq.10 for Kurra Chine A Unit is shown in Figure 12A.

$$ØNDcorr = (ØDcorr + ØNcorr)/2 \text{-------- Eq.10}$$

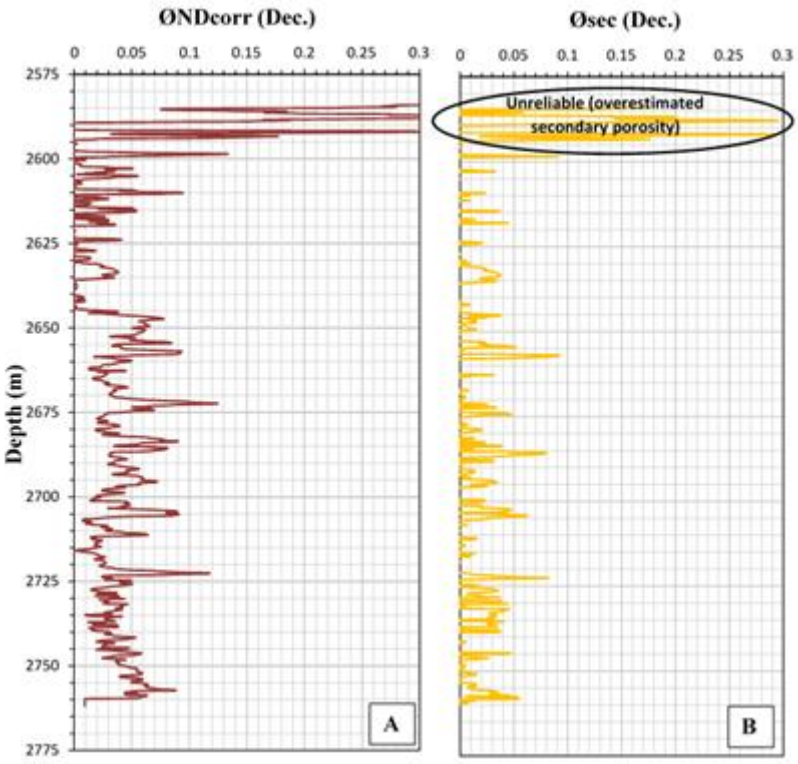

Fig. 12: A, Corrected Neutron-Density combination porosity (ØNDcorr); B, Secondary porosity (Øsec) for Kurra Chine A Unit in SH-4.

Zones of very low porosity (less than 1%) are concentrated at the upper part of the unit between depths 2595m and 2645m. The porosity at the middle and lower parts of the unit ranged generally between 2 and 8%.

In order to find out the contribution of fractures (as secondary porosity) in the total porosity of the formation, the difference between the calculated ØNDcorr and ØScorr measured and plotted as a curve in Figure 12B. The idea behind this method is that the recorded Δt by the tool of sonic log is represents the time taken by the first fast compressional wave passed through the matrix of the reservoir rock and ignoring the slower waves passed through the fractures, vuggs, or voids (secondary porosities).

Accordingly, the calculated porosity from Δt of sonic log is representing primary (matrix) porosity. In contrast to sonic logging tool, the porosity converted from the recorded ρb of density log and porosity recorded by neutron logging tool are both representing total porosity (primary and secondary).

Except the unreliable high secondary porosity values measured at the uppermost part of the formation, The contribution of fractures look to be generally less than 4% in most parts of the studied Kurra Chine A Unit. Zones with no fractures are also exist along the studied unit.

Mode of Shale Distribution: The relationship between ØD and ØN can aid in determining the mode of distribution for shale content within the pore spaces and around the grains. Based on the proposed crossplot by [20] for determining shale distribution mode in reservoirs, dispersed type appeared to be the dominant mode of shale distribution in the studied Kurra Chine A Unit in the well SH-4 (Fig.13).

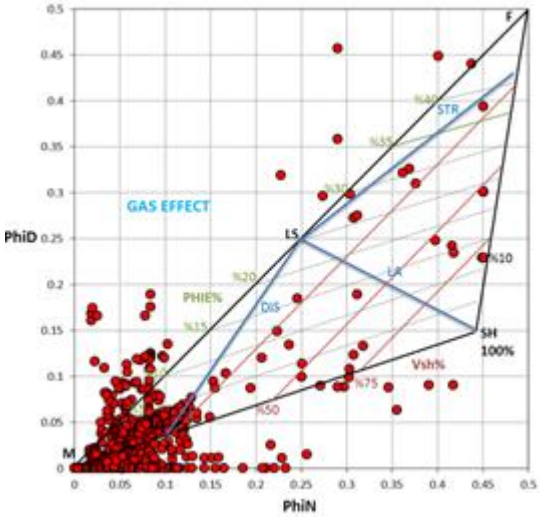

Fig. 13: Thomas-Stieber crossplot for determining mode of shale distribution for Kurra Chine A Unit in SH-4.

The crossplot also helps in correcting the porosity from effect of shale and that by determining the values of ØD and ØN for the adjacent shale bed (the point of SH100% on the crossplot) and considering the zero porosity line to be M-SH100%. Thus, the corrected porosity values for the studied unit look to be mostly less than 5%.

Hydrocarbon Saturation:

The available resistivity logs have been used for calculating water saturation of the studied unit (Fig. 14). The known Archie's formulas for calculation of water saturations in both un-invaded and flushed zones are applied (Eqs.11 and 12).

$$Sw = \sqrt[n]{\left(\frac{a}{\emptyset^m}\right) * \left(\frac{Rw}{Rt}\right)} \text{---------- Eq.11}$$

$$Sxo = \sqrt[n]{\left(\frac{a}{\emptyset^m}\right) * \left(\frac{Rmf}{Rxo}\right)} \text{--------- Eq.12}$$

Where:

Sw: Water saturation in the uninvaded zone (in fraction)

Sxo: Water saturation in the flushed zone (in fraction)

n: Saturation exponent (its value ranges from 1.8 to 2.5 but mostly equal to 2.0, the value used in this study)

a: Tortuosity factor (complexity of the paths and is equal to 1.0 for carbonates, the case of this study)

Ø: Porosity

m: Cementation exponent

Rw: Resistivity of formation water (in ohm.m)

Rt: True resistivity (in ohm.m)

Rmf: Resistivity mud filtrate (in ohm.m)

Rxo: Resistivity of flushed zone (in ohm.m)

The value of cementation exponent (m) has been calculated for Kurra Chine A Unit using Picket plot as shown in Figure 15, and appeared to be equal to 1.5.

Calculation of residual and movable hydrocarbon saturation done by applying equations Eq.13 and Eq.14 respectively.

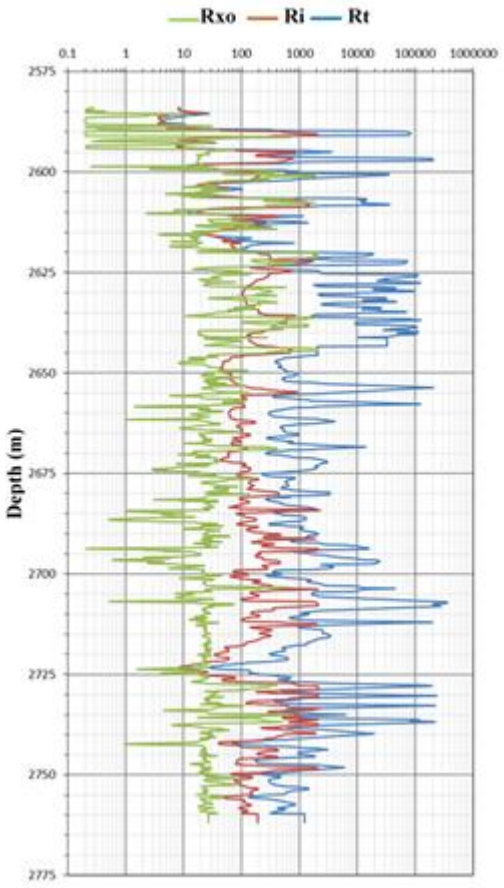

Fig. 14: Resistivity log record of Kurra Chine A Unit in SH-4.

$$Shr = 1 - Sxo \text{ ----------Eq.13}$$

$$Shm = 1 - Sw - Shr \text{ ----Eq.14}$$

Where:

Shr: Residual hydrocarbon saturation

Sxo: Water saturation in the flushed zone

Shm: Movable hydrocarbon saturation

Sw: Water saturation in the un-invaded zone

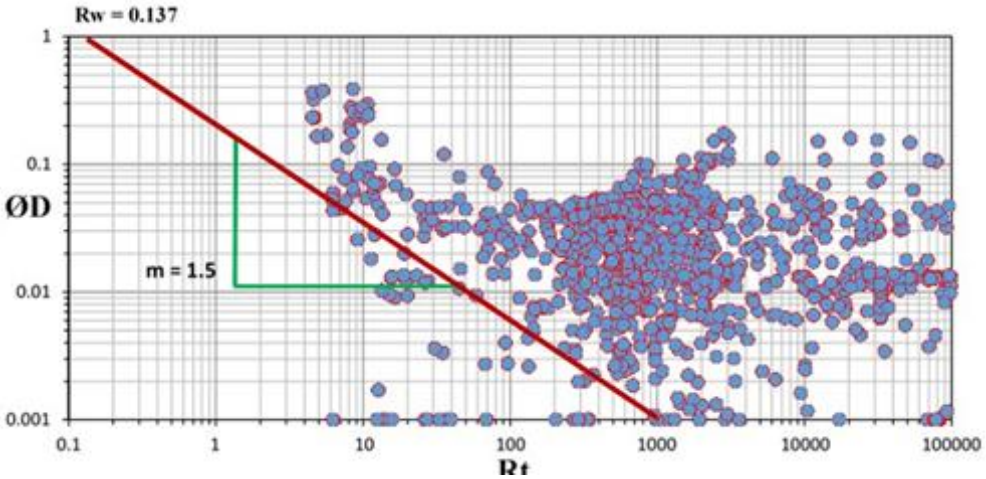

Fig. 15: Picket plot for determining cementation exponent (m) for Kurra Chine A Unit in SH-4.

The distribution of the Sw, Shr, and Shm within the frame of the porosity of the studied Kurra Chine A Unit is shown in Figure 16.

The general observations about the fluid saturations in Kurra Chine A Unit are:

- The unit contains hydrocarbons in its whole parts with different saturations
- The percentages of water saturation is higher at the upper part of the unit (from top of the
- formation to the depth 2625m), and that primly due to being the porosities too low and too small (high capillary pressure).
- The middle and the lower part of the unit are containing higher percentages of hydrocarbons (> 70%).
- There are movable hydrocarbons along the studied unit intercalated by narrow zones of non-movable hydrocarbons.
- The percentage of the residual hydrocarbon saturation is much higher than the percentage of the movable hydrocarbon saturation at the whole parts of the unit.

Permeability Calculation:

In order to find out values of permeability for the studied unit, an attempt done to take benefit from the core test done for a selected depth interval between 2642m and 2655m. The fuzzy method of combining between permeability values from core samples and values of the available.

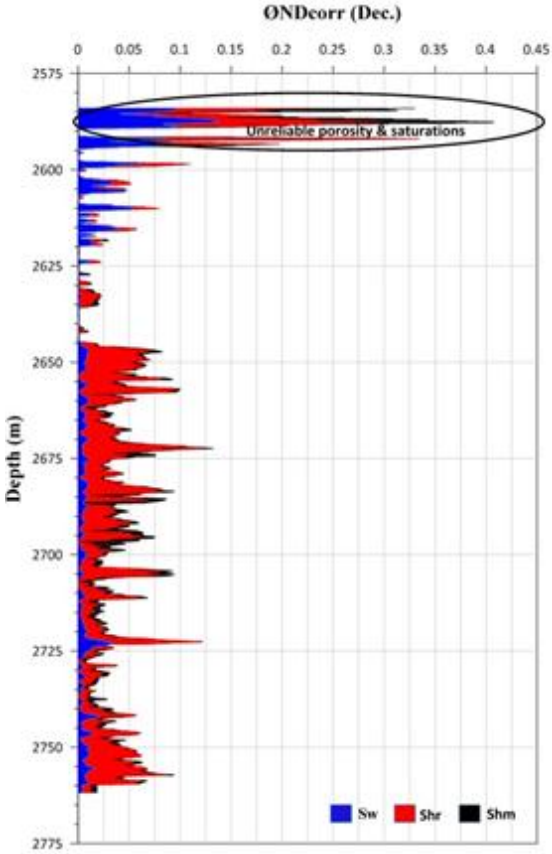

Fig. 16: Distribution of water, residual hydrocarbon, and movable hydrocarbon saturations within the pore spaces of Kurra Chine A Unit in SH-4 well.

logs (at the same depths of the core samples) is followed using Multiple Regression Analysis (MRA) method.

Unfortunately, no suitable equation obtained through the MRA method that best represent relationship between the core permeability values and the log readings. Accordingly, the core permeability replaced by permeability calculated through applying [21]'s equation (Eq. 14) for a selected depth interval at which water saturation values are less than 10% (at irreducible water saturation condition). Best equation representing permeability and the log readings of Gr, Δt, ρb, and ØN is find out to be Eq.15. Figure 17 shows the acceptable matching between the permeability values calculated through Schlumberger's equation (Eq.14) and those that obtained through the MRA equation (Eq.15).

$$K = 10000 * \left(\frac{\emptyset^{4.5}}{Swirr^2}\right) \text{ ------ Eq.14}$$

Permeability from log, K= 402.7299 + (-8.2819 x Gr) + (0.167773 x Δt) + (-122.703 x ρb) + (714.4979 x ØN) ------Eq.15

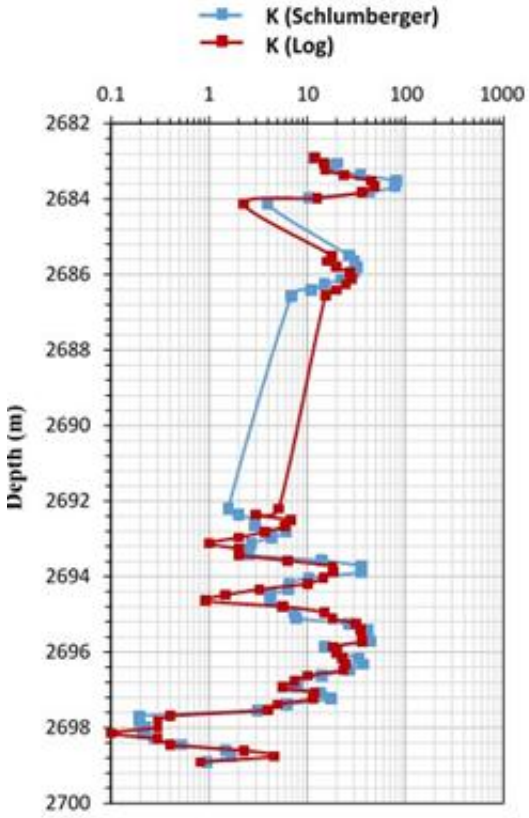

Fig. 17: Permeability estimation using Schlumberger equation and log data for a selected interval of Kurra Chine A Unit in the well SH-4.

Finally, permeability for the complete Kurra Chine A Unit calculated as shown in Figure 18. The studied unit appears to be containing a lot of impermeable intervals especially at the upper part. The impermeable intervals intercalated a lot of permeable zones with permeability values ranging between <1.0 and <100mD.

Most of the permeable intervals are concentrated at the lower part of the Unit. Permeable intervals

disappears gradually towards the upper part of the unit.

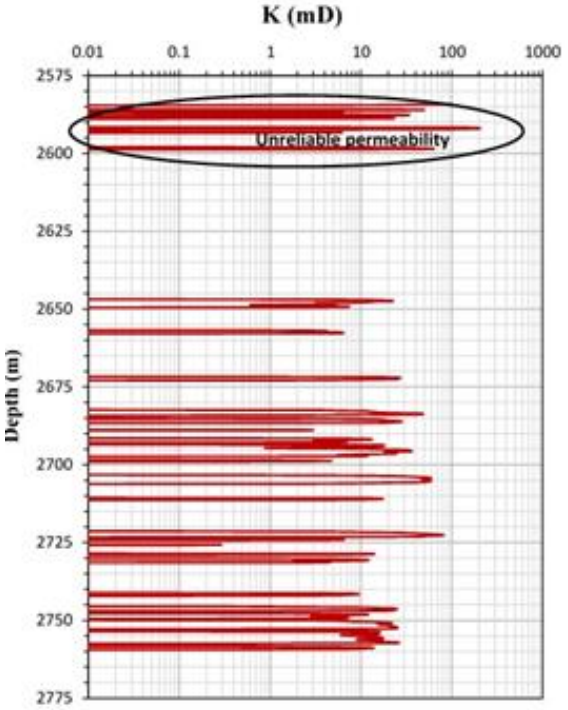

Fig. 18: Calculated Permeability (K) for the studied Kurra Chine A Unit in the well SH-4.

Reservoir Units:

As porosity and permeability are the main factors that determine efficiency of reservoirs, so, the calculated Vsh, ØNDcorr, and K are depended on to subdivide the studied unit to distinguished reservoir units.

Three reservoir units have been identified as shown in Figure 19. Reservoir unit-1 (RU-1) at the top of the studied unit, between depths 2577m and 2645m, is of lowest reservoir property.

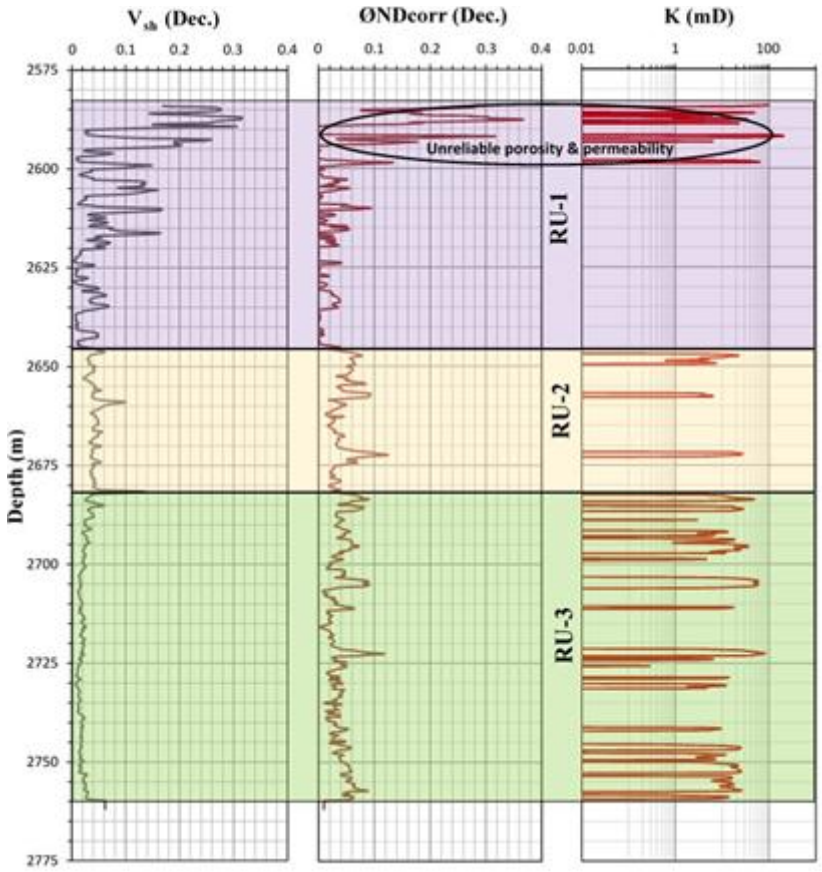

Fig. 19: Distinguished reservoir units for Kurra Chine A Unit in the well SH-4.

This reservoir unit has the highest shale content (about 30% in some intervals) and the lowest porosity (mostly <4%) with no permeable intervals or with less than 0.01mD permeability intervals. The upper part of this reservoir unit is composed mainly of shale and mudstone whereas its lower part is composed mainly of anhydrite and dolomitic anhydrite. RU-2 at the middle part of the studied unit, between depths 2645m and 2677m, contains about 5% shale and porosity ranging generally between 2% and 8%. Only three distinguished permeable intervals identified in this reservoir unit located at depth intervals 2645-2649m (0.8-30mD), 2656-2657m (about 17mD), and 2672-2673m (about 35mD). This unit consists of anhydritic dolomite, anhydrite, and dolomite interbedded with shale and mudstone.

RU-3 at the lower part of the studied unit, between depths 2677m and the base of unit at depth 2761m. This clean reservoir unit contains lowest shale content (about 2%) and porosity almost as RU-2 (generally ranging between 2% and 8%) but with a lot of permeable intervals intercalated with anhydritic impermeable or of less than 0.01 mD permeability zones. This unit is lithologicaly composed of dolomite, anhydritic dolomite, and anhydrite.

Hydrocarbon Movability and Flow Effeciency:

To show the flow effeciency in the studied unit based on the available log measured parameters, Flow Zone Indicator (FZI) proposed by [22] is applied. FZI is based on a modified Kozeny-Carmen equation and the concept of mean hydraulic radius. FZI is a unique parameter for each hydraulic flow unit which means that each distinct reservoir type has a unique FZI value. Hydraulic Flow Unit (HFU), on the other hand, is a continuous body over a specific reservoir volume that practically possesses consistent petrophysical and fluid properties, which uniquely characterize its static and dynamic communication with the wellbore [23].

To measure FZI, equations Eq.17-19 are applied.

$FZI = RQI/\emptyset z$---------- Eq.17

$RQI = 0.0134\ (K/\emptyset z)^{0.5}$-------Eq.18

$\emptyset z = \frac{\emptyset e}{1-\emptyset e}$ ----------Eq-19

Where:

FZI: Flow Zone Indicator in µm

RQI: Reservoir Quality Index

Øz: Normalized Porosity Index (pore volume to matrix volume ratio)

Øe: Effective porosity in Decimal

K : Permeability in mD

The calculated FZI for the studied Kurra Chine A Unit showed that there are four distinctive HFUs as systems of flow. The actual frequency of the measured FZI values shows that HFU-1 (of FZI <2.0) is the highest dominated flow unit among the four identified types and comprises about 80 % of the FZI points, whereas HFU-4(of FZI >10) is the lowest dominant and comprises about 3% of the measured FZI points (Fig.20).

FZI after all is representing the relationship between porosity and permeability. It's important to mention that not always highest porosity is associating highest permeability. Figure 21 shows that HFU-1 is of lowest porosity but with highest permeability, whereas HFU-4 is of highest porosity but with lowest permeability.

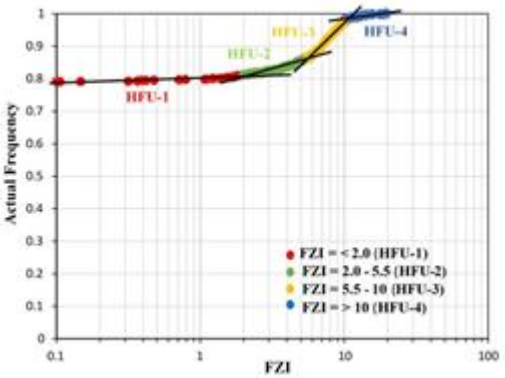

Fig. 20: Actual Frequency (distribution) of the calculated Flow Zone Indicators (FZI) for the studied Unit A of Kurra Chine Formation in the well SH-4 with the identified Hydraulic Flow Units (HFU).

So, porosity and permeability should be taken as a ratio (K/Ø) rather than be taken separately when flow efficiency of reservoirs is characterized.

As FZI shows only the flow effeciency in the term of porosity and permeability without any indications about the nature of the fluid that flows, therefore, to connect between flow and hydrocarbons, its vital to show zones where movable hydrocarbons are exist.

Movable Hydrocarbon Index (MHI) is one of the teqniques by which zones of movable hydrocarbons can be detected preliminarily within a reservoir and that depending on log data.

MHI represents the ratio of the water saturation in the un-invaded zone to water saturation (after invasion) at the flushed zone (Sw/Sxo), Eq.16.

$Sw/Sxo = \frac{Rxo/Rt}{Rmf/Rw}$ ------- Eq.16

As appears in Eq.16, for applying this technique no values of porosity and cementation exponent are needed.

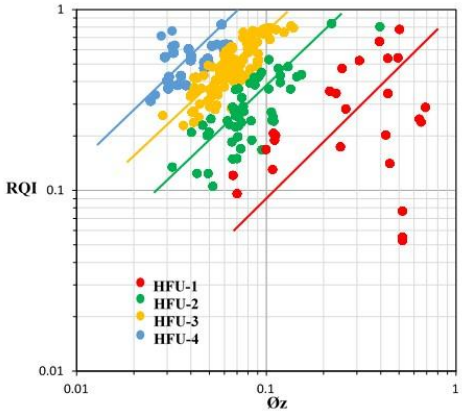

Fig. 21: Plot of RQI versus Øz for the studied Unit A of Kurra Chine Formation in the well SH-4 with the identified Hydraulic Flow Units (HFU).

Figure 22A is the plot of the calculated MHI for the studied Kurra Chine A Unit in the well SH-4 with the cutoff line of 0.6 which separates zones of movable hydrocarbons from zones of unmovable hydrocarbons for carbonate reservoirs [24]. The plot shows that the studied unit contains a lot of movable hydrocarbon zones especially within the RU-2 and RU-3 reservoir units.

The distribution of the four distinctive HFUs along the studied Kurra Chine A Unit (Fig.22B) is plotted along with the MHI plot to show best productive zones where movable hydrocarbon zones matches zones of highest FZI value (HFU-4).

RU-1, as expected, is of no or of lowest production potentiality, although movable hydrocarbon zones are exist within this unit.

Three zones of moderate production capacity identified in RU-2, separated by non-productive or by very low production potentiality zones.

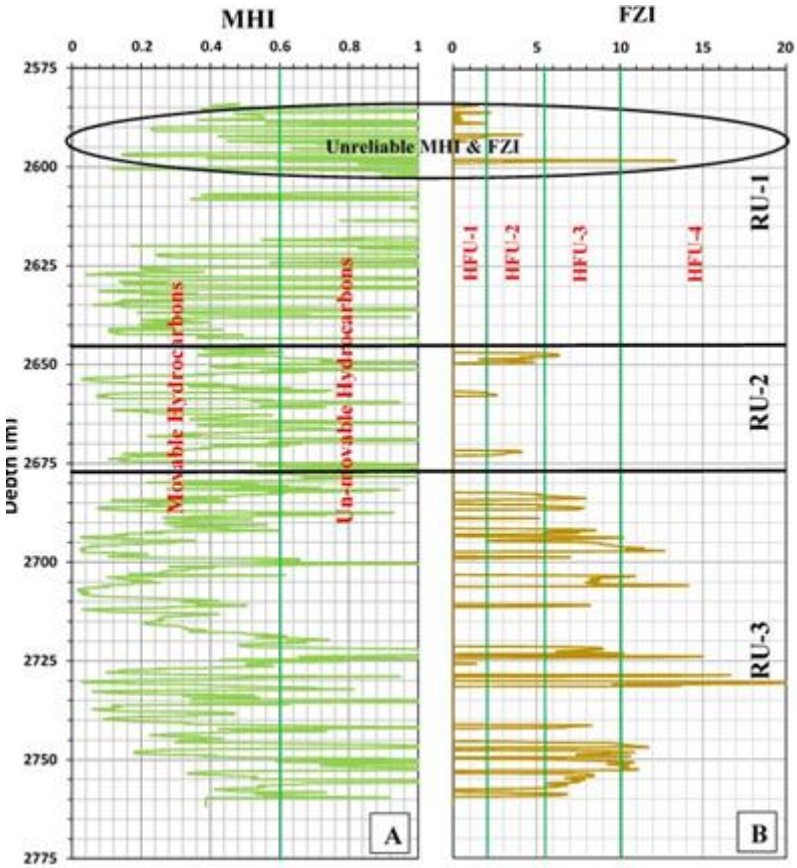

Fig. 22: A, Movable Hydrocarbon Index (MHI) and B, Flow Zone Indicator (FZI) for the distinguished reservoir units of Kurra Chine A Unit in the well SH-4.

The productive intervals of this reservoir unit located at the depths where considered in the previous sections as reservoir zones within RU-2 and collectively are about eight m thick (net pay).

About eight well productive zones identified in the RU-3 where less than 0.6 MHI values matched HFUs of greater than 10 FZI value. The best productive zone locates at the depth interval 2730-2732m. The total of 44m of this reservoir unit can be considered as net pay (with different capacities).

Accordingly, the net to gross (N/G) pay of RU-1 is expected to be almost 0%, RU-2 is about 25%, and of RU-3 is about 52%, and for the complete studied Kurra Chine A Unit is about 28%.

Conclusions

Unit A of Kurra Chine Formation in the well SH-4 composes mainly of dolomite, anhydritic dolomite, and anhydrite. The shale content is generally low but a slightly increase of shale content can be observed from the lower part upwards to be about 30% at the uppermost part of the unit. The porosity is also low especially at the upper part of the unit and is less than 5% in most parts of the unit. The secondary porosity at different depth levels comprises less than 4% of the total porosity. The shale content is distributed in a dispersed mode and composed primly of Illite and Chlorite. Hydrocarbons are exist in almost all parts of the unit but with higher percentages in the middle and lower part of the unit (higher than 70%). The greater percentage of the reservoired hydrocarbons are residual hydrocarbons. Most of the permeable intervals are concentrated at the middle and lower part of the unit and reaches to more than 70mD in some horizons. Kurra Chine A Unit consists of three reservoir units and four distinctive hydraulic flow units. Best productive intervals are exist at the RU-3 (lower part of the studied unit) with three productive intervals at the RU-2 (middle part of the studied unit)

and no observable productive interval at RU-1 (upper part of the studied unit). The total of 52m from the gross 184m of the studied unit can be considered as productive, which means that the G/N pay ratio for the studied Kurra Chine A Unit in SH-4 well is equal to about 28%.

Acknowledgments

Authors would like to thank so much Ministry of the Natural Resources/Iraqi Kurdistan Region, for providing the wireline log data used in this study.

References

[1] RPS Energy (2010). Evaluation of Shamaran Petroleum's interest in Atrush Block, Kurdistan, Available at (https://ekurd.net/wp-content/uploads/2018/12/Evaluation-of-Shamaran-petroleum-2010-Ekurd-net.pdf.

[2] Sadooni, F.N. (1995). Petroleum Prospects of Upper Triassic Carbonates in Northern Iraq. *Journal of Petroleum Geology*, **18** (**2**): 171-190.

[3] Al-Barzingy, S.J. (1999). Source Rocke Evaluation of Upper Triassic Kurra Chine Formation, Northwestern Iraq. Ph.D. thesis, Baghdad University, Baghdad, Iraq: 91p.

[4] Al-Ameri, T.K., Al-Dolaimy, Q.H., and Al-Khafaji, A.J. (2009). Palynofacies and Hydrocarbon Generation Potential of the Upper Triassic Kurra Chine Formation and lower part of the Baluti Formation, Mosul Block, Northwestern Iraq. *Arab Journal of Geosciences*, **2**: 273-283.

[5] Vulama, I. (2011). Source Rock Generative Potential and Volumetric Characteristics of the Kurra Chine Dolomite Formation, Hayan Block, Central Syrian Palmerides. *Geologia Croatica*, **64**(**3**): 259-272.

[6] Bellen, R.C., Dunnington, H.V., Wetzel, R. and Morton, D.M. (1959). Lexique Stratigraphique International. National de la recherché scientifique, 13, quai, Anatole-France, Paris: VII, 333p.

[7] Dunnington, H.V., Wetzel, R. and Morton, D.M. (1959). Mesozoic and Paleozoic. In: Bellen et al. (eds.), Lexique Stratigraphique International, v. 3, Asie, fascicle 10a, Centre National de la Recherche Scientifique: 1-133.

[8] Buday, P.T. (1980). The regional geology of Iraq: Tectonism, Magmatism and Metamorphism. State Establishment of Geological Survey and Mineral Investigation, Baghdad: Vol 1, 445p.

[9] Aqrawi, A.A.M., Goff, J.C, Horbury, A.D., and Sadooni, F.N. (2010). The petroleum geology of Iraq. Scientific Press Ltd, Beaconsfi eld, UK: 424 p.

[10] Sharland, P.R., Archer, R., Casey, D.M., Hall, S.H., Heward, A.P., Horbury, A.D., and Simmons, M.D. (2001). Arabian Plate Sequence Stratigraphy. *GeoArabia*, special publication 2, Gulf Petrolink, Bahrain: 371 p.

[11] Jassim, S.Z., Buday, T., Cicha, I., and Prouza, V. (2006). Late Permian-Liassic Megasequence AP6. In: Jassim S.Z., Goff, J. C., Geology of Iraq, publication of Dolin, Prague and Moravian Museum, Brno: 341p.

[12] Jassim, S.Z. and Goff, T. (2006). Phanerozoic development of the northern Arabian Plate, In: Jassim S.Z., Goff, J. C., Geology of Iraq, publication of Dolin, Prague and Moravian Museum, Brno: 341p.

[13] Kent, W.N. (2010). Structures of the Kirkuk Embayment, northern Iraq: Foreland structures or Zagros Fold Belt structures? *GeoArabia*, **15**(**4**):147-188.

[14] Al-Azzawi, N.K. and Hamdoon, A.N. (2008). Structure and Geomorphology of Shaikan Anticline-Northern Iraq. *Iraqi National Journal of Earth Science*, **8**(**1**): 54-63.

[15] GKS, 2020. Operations. Available at https://www.gulfkeystone.com/operations/

[16] Larionov, W.W. (1969). Borehole Radiometry: Nedra, Moscow, U.S.S.R.

[17] Ellis, D.V., and Singer, J.M. (2008). Well Logging for Earth Scientists, Second Edition, Springer, Dordrecht, Netherlands: 692p.

[18] Schlumberger (2009). Log Interpretation Charts. Sugar Land, Texas: 293p.

[19] Dewan, J. (1983). Essentials of Modern Open-Hole Log Interpretation: PennWell Publishing Company, Tulsa, Oklahoma: 361p.

[20] Thomas, E.C., and S.J. Stieber, S.J. (1975). The distribution of shale in sandstones and its effect on porosity. In: Trans. SPWLA 16th Annual Logging Symp. New Orleans, Louisiana: 4-7 June 1975.

[21] Schlumberger (2008). IP Interactive Petrophysics Vol. 3.5, Manual.

[22] Amaefule, J.O., Altunbay, M., Tiab, D., Kersey, D.G. and Keelan, D.K. (1993). Enhanced Reservoir Description: Using core and log data to identify hydraulic (flow) units and predict permeability in uncored Intervals/Wells", 68th Annual Tech. Conf. And Exhibit. Houston, TX
Paper SPE26435.

[23] Tiab, D. (2000). Advances in petrophysics, Vol. 1—flow units. Lecture notes manual, University of Oklahoma.

[24] Asquith, G. and Krygowski, D. (2004). Chapter 4: Porosity Logs. In: Asquith, G., and Krygowski, D. (eds.), Basic Well Log Analysis, (Second edition). AAPG Methods in exploration 16, Tulsa, Oklahoma: 37-76.

التقييم المكمني للوحدة A الكاربوناتي لتكوين قرة جيني الترياسي الأعلى في البئر SH-4 من حقل شيخان النفطي في كردستان العراق بأستخدام معطيات الجس البئري

دلير حسين بابان ، مصطفى محمد أحمد

قسم الجيولوجي ، كلية العلوم ، جامعة السليمانية ، السليمانية ، العراق

الملخص

تم دراسة الخواص المكمنية و كفاءة حركة الموائع للوحدة A من تكوين قرة جيني الترياسي الأعلى في البئر SH-4 من حقل شيخان النفطي في كردستان العراق و ذلك بأستخدام المتوفر من معطيات الجس البئري و نتائج الفحص المختبري لنماذج مختارة من اللباب. تتكون صخارية الوحدة A بصورة عامة من الدولومايت و الأنهايدرايت مع نسبة قليلة من السجيل في معظم أجزائها بأستثناء الجزء الأعلى من الوحدة حيث تتجاوز نسبة المحتوى السجيلي فيه 30%. كما تبلغ نسبة المسامية أقل من 5% في معظم أجزاء الوحدة المدروسة و لا تتجاوز نسبة المسامية الثانوية 4% من المسامية الكلية. تشكل الألّلايت و الكلورايت المعدنيين الطينيين الرئيسيين للمحتوى السجيلي الذي يتوزع على هيئة سجيل مبعثر في فراغات الصخرة المكمنية المدروسة. توجد الهايدروكاربونات تقريبا في كل أجزاء الوحدة A بنسبة تشبع تتجاوز 70% في الجزئين الأوسط و ألأسفل منها. لم يتم رصد وجود أنطقة نفاذة في الجزء الأعلى من الوحدة بينما لوحظ وجود عدة أنطقة نفاذة في الجزء الأسفل تجاوزت قيم نفاذية بعضها 70 ملليدارسي. يمكن تقسيم الوحدة A الى ثلاث وحدات مكمنية أعتمادا على التباين في نسب المحتوى السجيلي و قيم المسامية و النفاذية. فيما يخص حركة المائع فقد أظهرت دراسة دالة نطاق الجريان ان الوحدة قيد الدراسة تحتوي أربع وحدات جريان هيدروليكية مميزة ذات قيم لدالة نطاق الجريانمكونة من أقل من 2 ، 2–5.5 ، 5.5–10، و أكثر من 10. تم أحتساب نسبة العطاء الصافي الى السمك الكلي للوحدة A من تكوين قرة جيني و تبين انها تساوي 28% حيث بلغ سمك أنطقة العطاء مجتمعة حولي 52 مترا من السمك الكلي البالغ 184مترا.